Linear and cubic response to the initial eccentricity in heavy-ion collisions

Jacquelyn Noronha-Hostler,[1] Li Yan,[2] Fernando G. Gardim,[3] and Jean-Yves Ollitrault[2]

[1]*Department of Physics, Columbia University, New York, 10027, USA*
[2]*Institut de physique théorique, Université Paris Saclay, CNRS, CEA, F-91191 Gif-sur-Yvette, France*
[3]*Instituto de Ciência e Tecnologia, Universidade Federal de Alfenas,*
Cidade Universitária, 37715-400 Poços de Caldas, MG, Brazil
(Dated: November 13, 2015)

We study the relation between elliptic flow, v_2 and the initial eccentricity, ε_2, in heavy-ion collisions, using hydrodynamic simulations. Significant deviations from linear eccentricity scaling are seen in more peripheral collisions. We identify the mechanism responsible for these deviations as a cubic response, which we argue is a generic property of the hydrodynamic response to the initial density profile. The cubic response increases elliptic flow fluctuations, thereby improving agreement of initial condition models with experimental data.

I. INTRODUCTION

Anisotropic flow, v_n, in heavy-ion collisions is understood as the hydrodynamic response to the anisotropy of the initial density profile. In hydrodynamics, v_n is typically a functional of the initial density profile [1, 2]. For a given colliding system, energy, and centrality class, where the initial density profile fluctuates event to event, one can construct in every event predictors of elliptic flow, v_2, and triangular flow, v_3 using the initial anisotropies in the corresponding harmonics, ε_2 and ε_3 [1, 3, 4]. To a good approximation, v_2 and v_3 are determined by linear response to ε_2 and ε_3 [5–9].

Deviations from linear scaling of v_2 are however seen. In ideal hydrodynamics with a smooth, density profile, v_2/ε_2 increases slightly for peripheral collisions [10]. With a fluctuating initial density profile, the distribution of v_2 differs from the distribution of ε_2 for Pb-Pb collisions above 35% centrality [11]. This has been recently shown to result from a slight upward curvature of the relation between v_2 and ε_2 [12].

In Sec. II, we show that these deviations can be quantified by adding a cubic response term to the usual linear response. We study the variation of the response coefficients as a function of centrality in hydrodynamics. In Sec. III, we study the effect of the cubic response on elliptic flow fluctuations in relation with LHC data. In Sec. IV, we study the deviations between anisotropic flow and the predictor.

II. LINEAR AND CUBIC RESPONSE

In a hydrodynamic calculation of a relativistic heavy ion collision, particles are emitted independently from a fluid element, and all information is thus contained in the single-particle momentum distribution. This momentum distribution is determined by the initial conditions of the hydrodynamic evolution, that is, the initial energy density profile and the initial fluid velocity profile. The fluid velocity at early times is itself mostly determined by the energy density profile at earlier times [13, 14], as shown by direct inspection of hydrodynamic equations [15] and strong coupling calculations [16–18], so that all observables are to a very good approximation functionals of the sole initial density profile.

Anisotropic flow, v_n, is defined as the complex Fourier coefficient of the single-particle azimuthal distribution in an event, that is, $v_n \equiv \{e^{in\phi}\}$ [19] where $\{\cdots\}$ denotes an average over the freeze-out surface [20] of the fluid in a single event. We denote by ε_n the complex anisotropy in harmonic n [21], defined as

$$\varepsilon_n \equiv -\frac{\int r^n e^{in\phi}\epsilon(r,\phi)r\mathrm{d}r\mathrm{d}\phi}{\int r^n \epsilon(r,\phi)r\mathrm{d}r\mathrm{d}\phi}, \qquad (1)$$

where integration is over the transverse plane in polar coordinates, and $\epsilon(r,\phi)$ denotes the initial energy density at midrapidity. Note that the coordinate system must be centered, so that $\int re^{i\phi}\epsilon(r,\phi)r\mathrm{d}r\mathrm{d}\phi = 0$ in every event. Our study in this paper is restricted to the largest flow harmonics $n = 2, 3$. Other harmonics (v_1, v_4 and v_5) involve mode mixing through large nonlinear terms, which are already well understood [22, 23].

We write for a given initial geometry

$$v_n = f(\varepsilon_n) + \delta_n, \qquad (2)$$

where $f(\varepsilon_n)$ is an estimator of v_n based on the initial anisotropy ε_n, and δ_n is the residual, defined as the difference between the flow and the estimator. The estimator typically depends on a number of parameters (response coefficients). These parameters are fitted in order to minimize $\langle|\delta_n|^2\rangle$, where angular brackets denote averages over events in a centrality class. Note that $\delta_n = 0$ only if the estimator reproduces both the magnitude and phase of v_n [5]. In this respect, our procedure differs technically from that of Ref. [6], which only retains the information on the flow magnitude.

The eccentricity ε_n in a given harmonic transforms like v_n under azimuthal rotations. Therefore the estimator

$f(\varepsilon_n)$ must also transform like ε_n under azimuthal rotations. The simplest choice is

$$f(\varepsilon_n) = \kappa_n \varepsilon_n, \qquad (3)$$

corresponds to linear eccentricity scaling [1, 5]. The lowest nonlinear correction preserving rotational symmetry and analyticity is a cubic response term [7, 24]:

$$f(\varepsilon_n) = \kappa_n \varepsilon_n + \kappa_n' |\varepsilon_n|^2 \varepsilon_n, \qquad (4)$$

where κ_n is the linear response coefficient and κ_n' the cubic response coefficient. Parity requires that κ_n and κ_n' are both real. Their explicit expressions are derived in Appendix A. Note that the values of κ_n in Eqs. (3) and (4) differ in general, i.e., the linear response coefficient is modified by the cubic response.
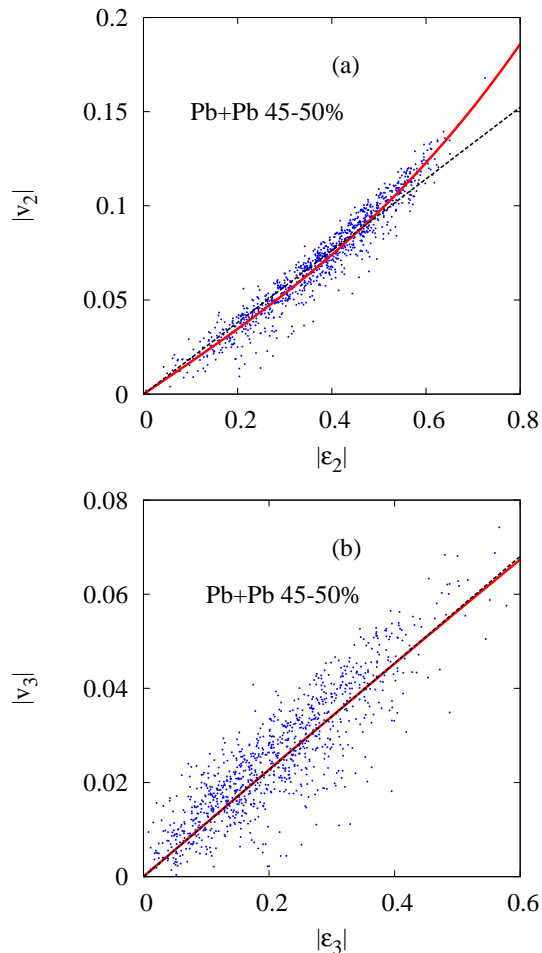

FIG. 1. (Color online) Correlation between the magnitudes of anisotropic flow v_n and initial eccentricity ε_n for Pb+Pb collisions at 2.76 TeV in the 45-50% centrality range. Each point corresponds to a different initial geometry. Dotted line: linear estimator, Eq. (3). Full line: cubic estimator, Eq. (4). (a) Elliptic flow. (b) Triangular flow.

We calculate v_n using the boost-invariant [25] 2+1 dimensional viscous relativistic hydrodynamical code v-USPhydro [26, 27]. The initial conditions are calculated using a Monte Carlo Glauber model [28–30] for Pb+Pb collisions at $\sqrt{s_{NN}} = 2.76$ TeV. The energy density at an initial time $\tau_0 = 0.6$ fm/c after the collision is assumed to be proportional to the density of binary collisions [31]. The centrality of the event is defined according to the number of participant nucleons [27]. For each 5% centrality class, we generate approximately 1000 events. We assume for simplicity that there is no initial transverse flow velocity $u^x = u^y = 0$, and that the bulk pressure, Π, and the shear stress tensor, $\pi^{\mu\nu}$, vanish at τ_0. We use a constant shear viscosity over entropy ratio $\eta/s = 1/4\pi$ [32, 33], and zero bulk viscosity. While a temperature dependent $\eta/s(T)$ and $\zeta/s(T)$ may be more realistic such as from [34, 35], it is unlikely that either would have a large impact on the results because the mapping is nearly identical between our constant η/s and the $\eta/s(T) + \zeta/s(T)$ from [7]. The equation of state is that of Ref. [36] with vanishing baryon chemical potential. We have adopted the popular quadratic ansatz for the viscous correction to the thermal distribution function [37, 38] and a constant freeze-out temperature $T_{FO} = 130$ MeV. We calculate v_n for pions emitted directly at freeze-out over the transverse momentum range $0.3 < p_t < 3$ GeV/c [39].

Fig. 1 displays scatter plots of the magnitudes of initial anisotropies $|\varepsilon_n|$ and anisotropic flow $|v_n|$ for $n = 2, 3$ in Pb+Pb collisions at 2.76 TeV in the 45-50% centrality range. The linear and cubic estimators (3) and (4) are also shown as dashed and solid lines, respectively. Note that these lines do not strictly correspond to best fits of the set of points: the magnitude of the best fit does not coincide with the best fit to the magnitudes (it is slightly lower), because the optimization of the estimator also involves the phases (see Appendix A for details). For elliptic flow, a clear departure from linear scaling is seen for large $|\varepsilon_2|$ [12], which is captured by the cubic term, and corresponds to a positive κ_2'. For triangular flow, such nonlinear effects are negligible. The dispersion of the results around the best-fit curve is studied in Sec. IV.

The values of κ_2 and κ_2' from Eq. (4) are displayed in Fig. 2 as a function of centrality. Statistical errors due to the finite number of events, shown as vertical bars in figures, are estimated by jackknife resampling [40]. A cubic response clearly appears above 10% centrality, although it is too small to be seen by visual inspection of the scatter plots below 40% centrality. While the linear response decreases with centrality, as expected as a consequence of viscous suppression [41], the cubic response *increases* with centrality, in such a way that the sum $\kappa_2 + \kappa_2'$ remains approximately constant (squares in Fig. 2). For sake of comparison, we have also carried out ideal hydrodynamic simulations for selected centrality bins (not shown). The linear response coefficient is larger than for viscous hydrodynamics, as expected, but the cubic coefficient is smaller: κ_2 and κ_2' again vary in opposite directions. We have also carried out calculations with MCKLN [42] initial conditions (not shown) and compared with the results from Glauber initial conditions.
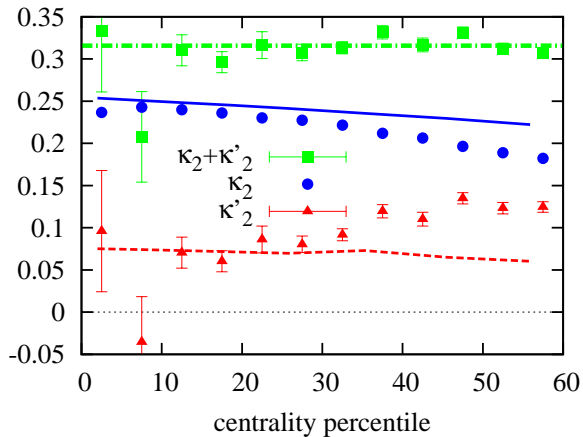
FIG. 2. (Color online) Response coefficients, as defined by Eqs. (4), for Pb+Pb collisions at $\sqrt{s_{NN}} = 2.76$ TeV, as a function of centrality percentile. Circles and solid line: linear response coefficient κ_2 with fluctuating and smooth initial conditions. Triangles and dashed line: cubic response coefficient κ_2' with fluctuating and smooth initial conditions. Squares: $\kappa_2 + \kappa_2'$. The dash-dotted horizontal line illustrates that $\kappa_2 + \kappa_2' \simeq 0.32$ for all centralities.

We find that the variations of κ_2 and κ_2' as a function of centrality are similar, but stronger: in particular, κ_2 becomes smaller than κ_2' for the most peripheral bin. The sum $\kappa_2 + \kappa_2'$ is also approximately constant.

In Eq. (2), one expects that the estimator $f(\varepsilon_2)$ captures the long-range structure of the initial density profile [1, 43, 44] while the residual δ_2 is driven by short-range structures. In order to test this hypothesis, we repeat the calculation with a smooth Gaussian initial density profile, for which one expects $\delta_2 \approx 0$.[1] In every centrality bin, we fix the total entropy and rms radius to the same value as in the previous calculation with fluctuating initial conditions. We calculate v_2 for two different values of ε_2 (0.15 and 0.25) and determine κ_2 and κ_2' by solving $v_2 = \kappa_2 \varepsilon_2 + \kappa_2' \varepsilon_2^3$. We use a third value of ε_2 (0.3) to check that results are compatible.

Our calculation with smooth initial conditions uses a different code [22] than the calculation with fluctuating initial conditions. The differences are the following. The shear tensor $\Pi^{\mu\nu}$ is initialized to the Navier-Stokes value, not to 0, but this is known to have a negligible effect at late times [45]. The equation of state is that of Ref. [46], but we have also checked that this has a negligible effect. Finally, the event-by-event calculations are done with the Lagrangian method known as Smoothed Particle Hydrodynamics [47, 48] while the smooth initial conditions are done within a grid method. However, both reproduce exact solutions [49] so the results should be comparable.

---

[1] In particular, the phase of δ_2 is exactly zero due to symmetry of the Gaussian.

The results with smooth initial conditions are shown as lines in Fig. 2. Up to 30% centrality, smooth initial conditions and fluctuating initial conditions give very similar results for both κ_2 and κ_2'. Above 30% centrality, the centrality dependence is stronger with fluctuating initial conditions than with smooth initial conditions. In particular, no increase of κ_2' with centrality percentile is observed with smooth initial conditions. This difference between smooth initial conditions and fluctuating initial conditions appears — as it should — when the size of the system is smaller and becomes comparable to the size of the fluctuations. We also find (not shown in figure) that the cubic response coefficient is slightly larger in ideal hydrodynamics than in viscous hydrodynamics, while the opposite variation is seen with fluctuating initial conditions.

Thus all our hydrodynamic calculations, ideal or viscous, with or without fluctuations confirm that a cubic response exists in addition to the well known linear response. The effect of the cubic response is negligible for central collisions but becomes sizable as the centrality percentile increases. Around 50% centrality, about 10% of the elliptic flow comes from the cubic term, hence the cubic response matters for precision studies.

For v_3, a similar analysis shows the relevant cubic response term is proportional to $|\varepsilon_2|^2 \varepsilon_3$, not $|\varepsilon_3|^2 \varepsilon_3$. Detailed results are presented in Appendix B.

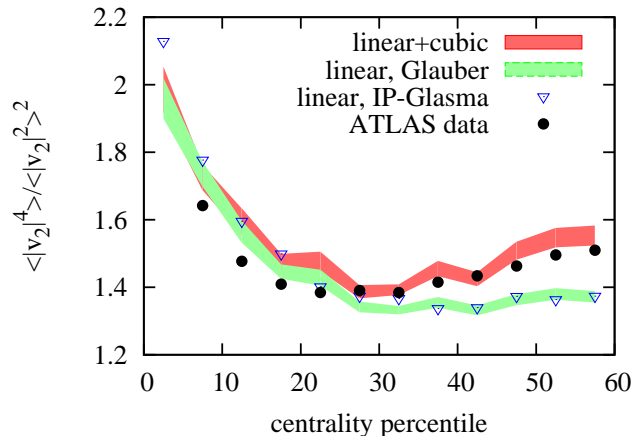## III. APPLICATION TO ELLIPTIC FLOW FLUCTUATIONS

FIG. 3. (Color online) Ratio $\langle v_2^4 \rangle / \langle v_2^2 \rangle^2$ for Pb+Pb collisions at $\sqrt{s_{NN}} = 2.76$ TeV as a function of centrality percentile. Light shaded band: assuming linear response, with Monte-Carlo Glauber initial conditions. Dark shaded banded: with cubic response added. Triangles: assuming linear response with IP Glasma initial conditions [11, 50]. Circles: ATLAS data [51].

We now discuss the effect of cubic response on ellip-

tic flow fluctuations. The magnitude of flow fluctuations can be quantified by ratios of cumulants [52, 53] or moments [54] of the distribution of v_2. The simplest ratio is [21] $\langle|v_2|^4\rangle/\langle|v_2|^2\rangle^2$, where angular brackets denote an average over events in a centrality class. Neglecting δ_n in Eq. (2), Eq. (4) gives, to leading order in the cubic response κ_2':

$$\frac{\langle|v_2|^4\rangle}{\langle|v_2|^2\rangle^2} \simeq \frac{\langle|\varepsilon_2|^4\rangle}{\langle|\varepsilon_2|^2\rangle^2}\left(1 + 4\frac{\kappa_2'}{\kappa_2}\left(\frac{\langle|\varepsilon_2|^6\rangle}{\langle|\varepsilon_2|^4\rangle} - \frac{\langle|\varepsilon_2|^4\rangle}{\langle|\varepsilon_2|^2\rangle}\right)\right). \quad (5)$$

The left-hand side differs from the right-hand side by less than 0.02 for all centralities, which means that the ratio of moments of the v_2 distribution is determined to an excellent approximation by the corresponding ratio of eccentricities, corrected by the cubic response.

When $\kappa_2' > 0$, the cubic response increases the ratio. The shaded bands in Fig. 3 display the right-hand side of Eq. (5) with and without the cubic response κ_2', for our Monte-Carlo Glauber model of initial conditions. With linear response alone, the ratio is slightly too large for central collisions and too low for peripheral collisions. The cubic response leaves the ratio unchanged for central collisions but increases it by up to 15% for peripheral collisions where it significantly improves agreement with experimental data [51].

In a previous hydrodynamic study using as initial condition the IP-Glasma model [11], it was found that the distribution of v_2 matches experimental data for all centralities while the distribution of ε_2 is too narrow for centralities above 35%. This observation is naturally explained by the cubic response. Figure 3 shows that the fluctuations of ε_2 are very similar with the IP-Glasma model and with the Monte-Carlo Glauber.

The fact that linear eccentricity scaling alone underpredicts the ratio for peripheral collisions has also been noted previously [21] using Monte-Carlo Glauber and MCKLN [42] models. It seems a generic feature of existing models of initial conditions. Once the cubic response is taken into account, one expects models to be in better agreement with data on elliptic flow fluctuations.

IV. RESIDUAL ANALYSIS

Figure 1 shows that there is a significant dispersion of anisotropic flow for a given initial anisotropy, i.e., a significant residual δ_n. For elliptic flow, the magnitude of δ_2 is typically 10% of the value of v_2, which is as large or larger than the cubic response. But unlike the cubic response, the residual averages to zero, so that its effect on measured quantities, which are averaged over many events, is small. For instance, its contribution to the mean square elliptic flow is proportional to $|\delta_2|^2$, as shown by Eq. (A3). Therefore, the correction from the residual to the rms value of v_2 is typically less than 1% in relative value.

The residual δ_n is due to short-range fluctuations
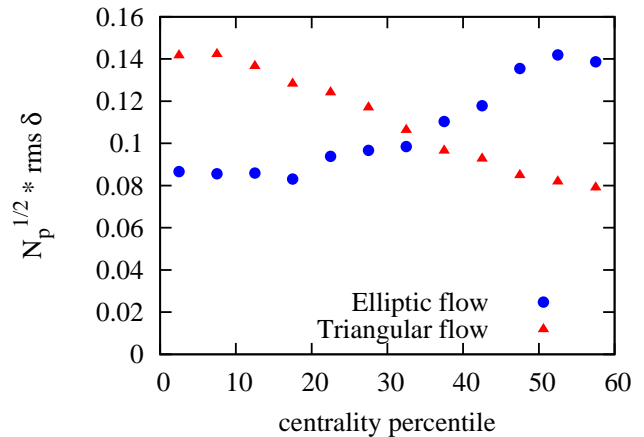

FIG. 4. (Color online) rms value of the residual δ_n multiplied by $N_p^{1/2}$, where N_p is the average number of participants in the centrality bin, as a function of centrality percentile, for the same viscous hydrodynamic calculation as in Fig. 2.

whose effect is not captured by the eccentricity ε_n. Fluctuations in our calculation are due to the finite number of participant nucleons N_p. Therefore one naturally expects that the magnitude of δ_n scales roughly like $N_p^{-1/2}$. Figure 4 displays $\sqrt{N_p\langle|\delta_n|^2\rangle}$ as a function of the centrality percentile from our viscous hydrodynamic calculation for $n = 2, 3$. One sees that it varies by less than a factor 2, while the number of participants varies almost by a factor 10. The decrease of $\langle|\delta_3|^2\rangle/\langle|\delta_2|^2\rangle$ as a function of centrality percentile seen in Fig. 4 can be ascribed to the larger damping of v_3, relative to v_2 [55].

We have checked that $\langle|\delta_n|^2|f_n|^2\rangle = \langle|\delta_n|^2\rangle\langle|f_n|^2\rangle$ within errors for all centralities. This means that the magnitude of the residual is independent of that of the estimator, a property referred to as *homoscedasticity*.

Finally, we have studied whether the distribution of δ_n is isotropic. The projection of δ_n parallel to the estimator $f(\varepsilon_n)$ corresponds to the dispersion in the magnitude $|v_n|$, while the projection perpendicular to $f(\varepsilon_n)$ corresponds to the dispersion in the flow angle. For elliptic flow, we find a sizable anisotropy as the centrality percentile increases: $\langle[\mathrm{Re}(\delta_2^* f(\varepsilon_2))]^2\rangle > \langle[\mathrm{Im}(\delta_2^* f(\varepsilon_2))]^2\rangle$, which means that the relative fluctuations of the flow magnitude with respect to the estimator are larger than the fluctuations of the flow angle.

V. CONCLUSIONS

We find that the elliptic flow not only has a contribution from the usual linear response from the initial eccentricities but there is a nonzero cubic response that plays a strong role for mid-central to peripheral collisions, which highlights the importance of cubic response for large eccentricities. In fact, its contribution to the to-

tal elliptic flow is of order 10% at around 50% centrality. The existence of non-zero cubic response indicates that the distribution of v_2 is not homothetic to the distribution of ε_2, as usually assumed [24, 56–59].

Because we consistently see this effect regardless of the scale of fluctuations and the type of viscosity, we conclude that it is a general property of the hydrodynamic response. Current calculations are for Pb+Pb collisions at $\sqrt{s_{NN}} = 2.76$ TeV, however, previous results at Au+Au RHIC energies [7] qualitatively appear to have nearly identical response. Most likely smaller, asymmetric systems would display similar effects but they may see a larger influence from small scale structure [60].

The sum of the linear and cubic response is approximately constant across centralities so one would naively expect a simple explanation. Note that this quantity corresponds (see Eq. (4)) to the limiting value of v_2 for $\varepsilon_2 \to 1$, i.e, to the emission from a one-dimensional source. While both smoothed and event-by-event initial conditions see a non-zero cubic response, the magnitude of the each is quite different across centralities. With fluctuating initial conditions, the cubic response coefficient, κ'_2 consistently increases as a function of centrality percentile whereas it is roughly constant for smoothed initial conditions. Thus, for event-by-event initial conditions the cubic response is large precisely in the region where the cubic response is most relevant. Conversely, the linear response coefficient, κ_2, decreases across centralities at a steeper rate for event-by-event fluctuations. We conclude then that the cubic response depends on the detailed structure of initial conditions with a non-trivial dependence on the small scale fluctuations of the initial density profile, which deserves further investigations.

ACKNOWLEDGMENTS

Appendix A: Expressions of response coefficients

If the estimator $f(\varepsilon_n)$ in Eq. (2) depends on a number of parameters, minimizing $\langle|\delta_n|^2\rangle$ with respect to these parameters gives the condition

$$\mathrm{Re}\langle(v_n - f(\varepsilon_n))\,df^*(\varepsilon_n)\rangle = \mathrm{Re}\langle\delta_n\,df^*(\varepsilon_n)\rangle = 0. \quad (A1)$$

Differentiating with respect to κ_n in Eq. (3) or Eq. (4) (keeping κ'_n/κ_n constant) gives $df \propto f$, and Eq. (A1)

gives

$$\mathrm{Re}\langle v_n f^*(\varepsilon_n)\rangle = \langle|f(\varepsilon_n)|^2\rangle. \quad (A2)$$

This equation allows to relate the difference $\langle|\delta_n|^2\rangle$ to the Pearson correlation coefficient between the flow v_n and the estimator $f(\varepsilon_n)$. Using Eq. (2) and Eq. (A2), one obtains

$$\langle|\delta_n|^2\rangle = \langle|v_n|^2\rangle - \langle|f(\varepsilon_n)|^2\rangle. \quad (A3)$$

The Pearson correlation coefficient is defined as

$$Q_n \equiv \frac{\mathrm{Re}\langle v_n f^*(\varepsilon_n)\rangle}{\sqrt{\langle|v_n|^2\rangle\langle|f(\varepsilon_n)|^2\rangle}} = \sqrt{\frac{\langle|f(\varepsilon_n)|^2\rangle}{\langle|v_n|^2\rangle}}, \quad (A4)$$

where, in the last equality, we have used Eq. (A2). Q_n lies between -1 and $+1$. Using this equation, Eq.(A3) gives

$$\frac{\langle|\delta_n|^2\rangle}{\langle|v_n|^2\rangle} = 1 - Q_n^2. \quad (A5)$$

When Q_n is close to 1, the difference between the flow and the estimator is small, as expected.

With a purely linear response, Eq. (3), the expression of the coefficient is [5]

$$\kappa_n = \frac{\mathrm{Re}\left(\langle v_n \varepsilon_n^*\rangle\right)}{\langle|\varepsilon_n|^2\rangle}. \quad (A6)$$

When a cubic response term is added, Eq. (4), one must minimize $\langle|\delta_n|^2\rangle$ with respect to κ_n and κ'_n. This yields a system of two equations whose solution is

$$\kappa_n = \frac{\mathrm{Re}\left(\langle|\varepsilon_n|^6\rangle\langle v_n \varepsilon_n^*\rangle - \langle|\varepsilon_n|^4\rangle\langle v_n \varepsilon_n^*|\varepsilon_n|^2\rangle\right)}{\langle|\varepsilon_n|^6\rangle\langle|\varepsilon_n|^2\rangle - \langle|\varepsilon_n|^4\rangle^2}$$
$$\kappa'_n = \frac{\mathrm{Re}\left(-\langle|\varepsilon_n|^4\rangle\langle v_n \varepsilon_n^*\rangle + \langle|\varepsilon_n|^2\rangle\langle v_n \varepsilon_n^*|\varepsilon_n|^2\rangle\right)}{\langle|\varepsilon_n|^6\rangle\langle|\varepsilon_n|^2\rangle - \langle|\varepsilon_n|^4\rangle^2}. \quad (A7)$$

Note that the expression of the linear response coefficient κ_n is modified by including a cubic response. On the other hand, the cubic response only increases the Pearson coefficient Q_n by a negligible amount.

Appendix B: Triangular flow

We have carried out the same analysis for v_3 as for v_2. With fluctuating initial conditions, the cubic response κ'_3 defined in Eq. (4) is compatible with zero within statistical error bars, as seen in Fig. 5. Considering all centralities together, a negative value is preferred. We have also tested a different type of cubic response mixing the second and third harmonic, namely:

$$v_3 = \kappa_3\varepsilon_3 + \kappa'_{23}|\varepsilon_2|^2\varepsilon_3 + \delta_3. \quad (B1)$$

Since $|\varepsilon_2|$ is significantly larger than $|\varepsilon_3|$ for mid-central collisions, one expect that such a term could be larger
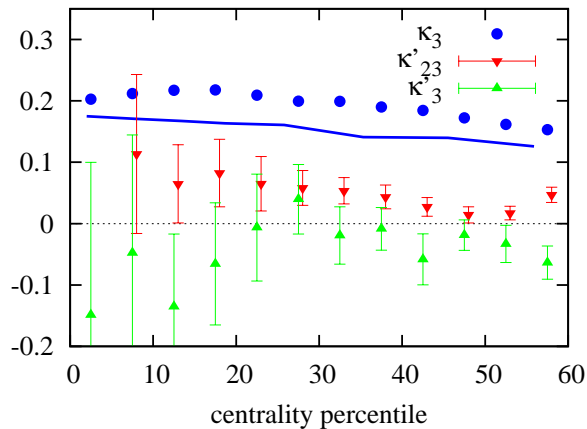
FIG. 5. (Color online) Linear and cubic response coefficients, as defined by Eqs. (4), for triangular flow. Solid line and full circles: κ_3 with smooth and fluctuating initial conditions. Triangles: κ_3' and κ_{23}' (see Eq.(B1)) with fluctuating initial conditions.

than a cubic term involving just ε_3. The values of κ_{23}' are plotted in Fig. 5 as a function of centrality. Considering all centralities together, there is significant evidence for a small positive $\kappa_{23}' \sim 0.03$.

Figure 5 also presents our results for the linear response κ_3. Its value is essentially the same whether or not one includes cubic terms in the fit. It varies less than κ_2 as a function of centrality. We have also carried out a calculation with smooth initial conditions obtained by a triangular deformation of a symmetric Gaussian [1]. The resulting values of κ_3, shown as a solid curve in Fig. 5, are close to those obtained with fluctuating initial conditions.

[1] D. Teaney and L. Yan, Phys. Rev. C **83**, 064904 (2011) [arXiv:1010.1876 [nucl-th]].

[2] S. Floerchinger and U. A. Wiedemann, Phys. Lett. B **728**, 407 (2014) [arXiv:1307.3453 [hep-ph]].

[3] B. Alver *et al.* [PHOBOS Collaboration], Phys. Rev. Lett. **98**, 242302 (2007) [nucl-ex/0610037].

[4] B. Alver and G. Roland, Phys. Rev. C **81**, 054905 (2010) [Phys. Rev. C **82**, 039903 (2010)] [arXiv:1003.0194 [nucl-th]].

[5] F. G. Gardim, F. Grassi, M. Luzum and J. Y. Ollitrault, Phys. Rev. C **85**, 024908 (2012) [arXiv:1111.6538 [nucl-th]].

[6] H. Niemi, G. S. Denicol, H. Holopainen and P. Huovinen, Phys. Rev. C **87**, no. 5, 054901 (2013) [arXiv:1212.1008 [nucl-th]].

[7] F. G. Gardim, J. Noronha-Hostler, M. Luzum and F. Grassi, Phys. Rev. C **91**, no. 3, 034902 (2015) [arXiv:1411.2574 [nucl-th]].

[8] S. Plumari, G. L. Guardo, F. Scardina and V. Greco, arXiv:1507.05540 [hep-ph].

[9] J. Fu, Phys. Rev. C **92**, no. 2, 024904 (2015).

[10] R. S. Bhalerao, J. P. Blaizot, N. Borghini and J. Y. Ollitrault, Phys. Lett. B **627**, 49 (2005) [nucl-th/0508009].

[11] B. Schenke, P. Tribedy and R. Venugopalan, Nucl. Phys. A **926**, 102 (2014) [arXiv:1312.5588 [hep-ph]].

[12] H. Niemi, K. J. Eskola and R. Paatelainen, arXiv:1505.02677 [hep-ph].

[13] M. Habich, J. L. Nagle and P. Romatschke, Eur. Phys. J. C **75**, no. 1, 15 (2015) [arXiv:1409.0040 [nucl-th]].

[14] J. Liu, C. Shen and U. Heinz, Phys. Rev. C **91**, no. 6, 064906 (2015) [Phys. Rev. C **92**, no. 4, 049904 (2015)] [arXiv:1504.02160 [nucl-th]].

[15] J. Vredevoogd and S. Pratt, Phys. Rev. C **79**, 044915 (2009) [arXiv:0810.4325 [nucl-th]].

[16] W. van der Schee, Phys. Rev. D **87**, no. 6, 061901 (2013) [arXiv:1211.2218 [hep-th]].

[17] P. Romatschke and J. D. Hogg, JHEP **1304**, 048 (2013) [arXiv:1301.2635 [hep-th]].

[18] W. van der Schee, P. Romatschke and S. Pratt, Phys. Rev. Lett. **111**, no. 22, 222302 (2013) [arXiv:1307.2539].

[19] M. Luzum, J. Phys. G **38**, 124026 (2011) [arXiv:1107.0592 [nucl-th]].

[20] C. Gale, S. Jeon and B. Schenke, Int. J. Mod. Phys. A **28**, 1340011 (2013) [arXiv:1301.5893 [nucl-th]].

[21] R. S. Bhalerao, M. Luzum and J. Y. Ollitrault, Phys. Rev. C **84**, 034910 (2011) [arXiv:1104.4740 [nucl-th]].

[22] D. Teaney and L. Yan, Phys. Rev. C **86**, 044908 (2012) [arXiv:1206.1905 [nucl-th]].

[23] L. Yan and J. Y. Ollitrault, Phys. Lett. B **744**, 82 (2015) [arXiv:1502.02502 [nucl-th]].

[24] L. Yan, J. Y. Ollitrault and A. M. Poskanzer, Phys. Lett. B **742**, 290 (2015) [arXiv:1408.0921 [nucl-th]].

[25] J. D. Bjorken, Phys. Rev. D **27**, 140 (1983).

[26] J. Noronha-Hostler, G. S. Denicol, J. Noronha, R. P. G. Andrade and F. Grassi, Phys. Rev. C **88**, 044916 (2013) [arXiv:1305.1981 [nucl-th]].

[27] J. Noronha-Hostler, J. Noronha and F. Grassi, Phys. Rev. C **90**, no. 3, 034907 (2014) [arXiv:1406.3333 [nucl-th]].

[28] M. L. Miller, K. Reygers, S. J. Sanders and P. Steinberg, Ann. Rev. Nucl. Part. Sci. **57**, 205 (2007) [nucl-ex/0701025].

[29] B. Alver, M. Baker, C. Loizides and P. Steinberg, arXiv:0805.4411 [nucl-ex].

[30] M. Rybczynski, G. Stefanek, W. Broniowski and P. Bozek, Comput. Phys. Commun. **185**, 1759 (2014) [arXiv:1310.5475 [nucl-th]].

[31] T. Hirano and Y. Nara, Phys. Rev. C **79**, 064904 (2009) [arXiv:0904.4080 [nucl-th]].

[32] G. Policastro, D. T. Son and A. O. Starinets, Phys. Rev. Lett. **87**, 081601 (2001) [hep-th/0104066].

[33] P. Kovtun, D. T. Son and A. O. Starinets, Phys. Rev.

Lett. **94**, 111601 (2005) [hep-th/0405231].

[34] J. Noronha-Hostler, J. Noronha and C. Greiner, Phys. Rev. Lett. **103**, 172302 (2009) [arXiv:0811.1571 [nucl-th]].

[35] H. Niemi, G. S. Denicol, P. Huovinen, E. Molnar and D. H. Rischke, Phys. Rev. Lett. **106**, 212302 (2011) [arXiv:1101.2442 [nucl-th]].

[36] P. Huovinen and P. Petreczky, Nucl. Phys. A **837**, 26 (2010) [arXiv:0912.2541 [hep-ph]].

[37] D. Teaney, Phys. Rev. C **68**, 034913 (2003) [nucl-th/0301099].

[38] K. Dusling, G. D. Moore and D. Teaney, Phys. Rev. C **81**, 034907 (2010) [arXiv:0909.0754 [nucl-th]].

[39] S. Chatrchyan *et al.* [CMS Collaboration], Phys. Rev. C **87**, no. 1, 014902 (2013) [arXiv:1204.1409 [nucl-ex]].

[40] B. Efron, Ann. Stat. **7**, 1 (1979).

[41] H. J. Drescher, A. Dumitru, C. Gombeaud and J. Y. Ollitrault, Phys. Rev. C **76**, 024905 (2007) [arXiv:0704.3553 [nucl-th]].

[42] H.-J. Drescher and Y. Nara, Phys. Rev. C **75**, 034905 (2007) [nucl-th/0611017].

[43] R. S. Bhalerao, M. Luzum and J. Y. Ollitrault, Phys. Rev. C **84**, 054901 (2011) [arXiv:1107.5485 [nucl-th]].

[44] J. P. Blaizot, W. Broniowski and J. Y. Ollitrault, Phys. Lett. B **738**, 166 (2014) [arXiv:1405.3572 [nucl-th]].

[45] M. Luzum and P. Romatschke, Phys. Rev. C **78**, 034915 (2008) [Phys. Rev. C **79**, 039903 (2009)] [arXiv:0804.4015 [nucl-th]].

[46] M. Laine and Y. Schroder, Phys. Rev. D **73**, 085009 (2006) [hep-ph/0603048].

[47] C. E. Aguiar, T. Kodama, T. Osada and Y. Hama, J. Phys. G **27**, 75 (2001) [hep-ph/0006239].

[48] Y. Hama, T. Kodama and O. Socolowski, Jr., Braz. J. Phys. **35**, 24 (2005) [hep-ph/0407264].

[49] H. Marrochio, J. Noronha, G. S. Denicol, M. Luzum, S. Jeon and C. Gale, Phys. Rev. C **91**, no. 1, 014903 (2015) [arXiv:1307.6130 [nucl-th]].

[50] B. Schenke, P. Tribedy and R. Venugopalan, Phys. Rev. Lett. **108**, 252301 (2012) [arXiv:1202.6646 [nucl-th]].

[51] G. Aad *et al.* [ATLAS Collaboration], Eur. Phys. J. C **74**, no. 11, 3157 (2014) [arXiv:1408.4342 [hep-ex]].

[52] N. Borghini, P. M. Dinh and J. Y. Ollitrault, Phys. Rev. C **64**, 054901 (2001) [nucl-th/0105040].

[53] A. Bilandzic, R. Snellings and S. Voloshin, Phys. Rev. C **83**, 044913 (2011) [arXiv:1010.0233 [nucl-ex]].

[54] R. S. Bhalerao, J. Y. Ollitrault and S. Pal, Phys. Lett. B **742**, 94 (2015) [arXiv:1411.5160 [nucl-th]].

[55] B. H. Alver, C. Gombeaud, M. Luzum and J. Y. Ollitrault, Phys. Rev. C **82**, 034913 (2010) [arXiv:1007.5469 [nucl-th]].

[56] G. Aad *et al.* [ATLAS Collaboration], JHEP **1311**, 183 (2013) [arXiv:1305.2942 [hep-ex]].

[57] E. Retinskaya, M. Luzum and J. Y. Ollitrault, Phys. Rev. C **89**, no. 1, 014902 (2014) [arXiv:1311.5339 [nucl-th]].

[58] T. Renk and H. Niemi, Phys. Rev. C **89**, no. 6, 064907 (2014) [arXiv:1401.2069 [nucl-th]].

[59] M. Rybczynski and W. Broniowski, arXiv:1510.08242 [nucl-th].

[60] J. Noronha-Hostler, J. Noronha and M. Gyulassy, arXiv:1508.02455 [nucl-th].